Protein & Cell 2010, 1(1): 96–105
DOI 10.1007/s13238-010-0012-3

Protein & Cell

RESEARCH ARTICLE

Crystal structure of cytotoxin protein suilysin from *Streptococcus suis*

Lingfeng Xu[1*], Bo Huang[1*], Huamao Du[2,3], Xuejun C. Zhang[4], Jianguo Xu[3] (✉), Xuemei Li[1] (✉), Zihe Rao[1]

[1] National Laboratory of Biomacromolecules, Institute of Biophysics, Chinese Academy of Sciences, 15 Datun Road, Beijing 100101, China
[2] College of Biotechnology, Southwest University, Chongqing 400715, China
[3] State Key Laboratory for Infectious Disease Prevention and Control, National Institute for Communicable Disease Control and Prevention, Beijing 102200, China
[4] Protein Studies Program, Oklahoma Medical Research Foundation, 825 N.E. 13th street, Oklahoma City, OK 73104, USA

✉ Correspondence: xujg@public.bta.net.cn (J. Xu), lixm@sun5.ibp.ac.cn (X. Li)
Received November 4, 2009; accepted November 13, 2009

ABSTRACT

Cholesterol-dependent cytolysins (CDC) are pore forming toxins. A prototype of the CDC family members is perfringolysin O (PFO), which directly binds to the cell membrane enriched in cholesterol, causing cell lysis. However, an exception of this general observation is intermedilysin (ILY) of *Streptococcus intermedius*, which requires human CD59 as a receptor in addition to cholesterol for its hemolytic activity. A possible explanation of this functional difference is the conformational variation between the C-terminal domains of the two toxins, particularly in the highly conserved undecapeptide termed tryptophan rich motif. Here, we present the crystal structure of suilysin, a CDC toxin from the infectious swine pathogen Streptococcus suis. Like PFO, suilysin does not require a host receptor for hemolytic activity; yet the crystal structure of suilysin exhibits a similar conformation in the tryptophan rich motif to ILY. This observation suggests that the current view of the structure-function relationship between CDC proteins and membrane association is far from complete.

KEYWORDS suilysin, cholesterol-dependent cytolysin, crystal structure

INTRODUCTION

Streptococcus suis is a serious pig-infectious pathogen that causes arthritis, septicemia, meningitis and pneumonia, and has a detrimental impact on pork industries world-wide (Gottschalk and Segura, 2000). Suilysin secreted from *S. suis* was first characterized as a hemolysin fifteen years ago (Jacobs et al., 1994) and is considered as an important virulence factor of the pathogenesis (Gottschalk and Segura, 2000). This 497 amino acid residue protein belongs to the cholesterol-dependent cytolysin (CDC) family (Jacobs et al., 1994). Like other members of the CDC family produced by Gram-positive bacteria (Tweten et al., 2001), suilysin is secreted as a water soluble monomer and is able to lyse mammalian erythrocyte by punching holes on membranes of the target cells (Jacobs et al., 1994).

The mechanism of pore formation of CDC proteins has been intensively investigated. As a prototype of this family, perfringolysin O (PFO) has been studied in depth using X-ray crystallography, cryo-electron microscopy, mutagenesis analysis as well as other functional studies, through which a picture of the pore formation mechanism is emerging (Rossjohn et al., 1997; Tilley et al., 2005; Tweten, 2005). A CDC protein usually contains an N-terminal portion (i.e., domains 1 and 3), a connection domain (domain 2), and a

[*] These authors contributed equally to this work.

© Higher Education Press and Springer-Verlag Berlin Heidelberg 2010

C-terminal domain (domain 4). Domain 4 appears responsible for initial binding with the target cell membrane (Rossjohn et al., 1997). After binding to a cholesterol-rich membrane, monomers of CDC proteins undergo a series of conformational changes and oligomerize into a ring shaped prepore. It is followed by a transformation of several helices in domain 3 to β hairpins to complete the transmembrane pore formation (Tweten, 2005). Because of high similarity among primary sequences of CDC family members, the above mechanism is likely to be shared by the entire CDC family. More importantly, a recent study on the crystal structure of MACPF (membrane attack complex/performing) protein illustrates a clear folding similarity between MACPF and the N-terminal portion of PFO, suggesting that a CDC-like killing mechanism is also shared by the mammalian immune system against bacterial infection (Rosado et al., 2007).

In addition to the pore-formation mechanism, researchers are also interested in mechanisms of membrane recognition by CDC proteins, particularly their cholesterol dependency. It was thought for long time that cholesterol serves as a receptor that mediates the binding of a highly conserved undecapeptide (also called tryptophan rich motif) located in domain 4 to the membrane (Rossjohn et al., 1997, 2007). However, discovery and studies on intermedilysin (ILY) from *Streptococcus intermedius* forced people to rethink the role of by cholesterol. Unlike PFO, ILY specifically binds to human cells by recognizing human CD59 as a receptor (Nagamune et al., 1996; Giddings et al., 2004). Meanwhile, depletion of cholesterol from human erythrocytes traps ILY in the prepore form instead of affects nothing or totally abolishes the binding (Giddings et al., 2003). In addition, recent studies on ILY and PFO showed that cholesterol mediates the binding of three other small loops in domain 4, but not the Trp-rich motif, to the membrane (Soltani et al., 2007b). On the other hand, 3D structure comparison showed that those loops whose binding to membrane is mediated by cholesterol have nearly identical conformations between the PFO and ILY; and the only recognizable conformational difference between their 4th domains is located in the Trp-rich motif. Therefore, it was thought that a key factor affecting the membrane association of the C-terminal 4th domain is the conformation of its Trp-rich motif, which might also help explain the ILY specificity towards human erythrocytes (Soltani et al., 2007b). However, the molecular basis of such a structure-function relationship remains to be clarified.

Herein we report a 2.85 Å resolution crystal structure of a suilysin variant containing a point mutation in the 1st domain. While cholesterol is sufficient to trigging the membrane binding of suilysin as it does for PFO, the Trp-rich motif adopts an ILY-like "extended" conformation in the crystal structure of suilysin. This observation appears to challenge the hypothesis that the Trp-rich motif conformation is the structural determinant for membrane binding specificity.

RESULTS

Suilysin crystallization and structure determination

Recombinant proteins of full length suilysin (GenBank ID: 5099791, residues 1–497) from *Streptococcus suis* and a point mutation variant, Pro353 to Leu (P353L), were over-expressed in *Escherichia coli* at comparable yields. The P353L mutant was originally selected through error prone PCR and a functional screening (H.D., to be published). While WT suilysin crystals diffracted poorly, the mutant was crystallized and resulted in 2.85 Å resolution diffraction data. Therefore, subsequent X-ray crystallography analysis was performed on this P353L mutant suilysin; and in the following we do not make an explicit distinction between the WT and P353L variant of suilysin unless specifically indicated. The initial phases of the suilysin crystal were determined using the Se-Met based multiple-wavelength anomalous dispersion method (MAD). The crystal form belongs to space group $P3_121$. There is one suilysin molecule per asymmetric unit with a 56% solvent content (Matthews coefficient, V_M= 2.8 Å^3/Da) (Matthews, 1968). The crystal structure model was refined to R-working 27.9% (R-free 29.4%) and had an overall good geometry. The final model consisted of residues 32–242, 245–499 (Leu498 and Glu499 were adopted from the expression vector and will be omitted from the following discussion), seven water molecules, one 1,2,3-heptanetriol isomer H molecule, and one 1,1,1,3,3,3-hexafluoro-2-propanol molecule, the latter two of which were included in the crystallization solution as additives. Statistics of data collection and refinement are summarized in Table 1.

Overall structure

Suilysin monomer is a β-strand rich protein of an elongated rod-like shape with dimensions of 40 Å×53 Å×120 Å. About 43% of the whole structure is composed of 21 β-strands with lengths ranging from 5 to 31 amino acid residues. Another 14% structure consists of ten α-helices varying from 4 to 16 residues in length. Based on structural description of homologous proteins (Rossjohn et al., 1997), suilysin is divided into four domains (Fig. 1A). All α helices and β strands, which are conserved in 3D structure level among available CDC crystal structures (i.e., PFO, ILY, ALO and suilysin), are named hereafter based on domains where they reside and are listed in Fig. 2A.

Among the four domains of suilysin, domains 1–3 are discontinuous in the primary sequence. The global domain 1 (i.e., residues 32–48, 85–175, 226–271 and 347–370) has a 6-stranded antiparallel β-sheet. The longest α helix, ^{1}α3 (i.e., residues 147–162), and the point mutation site, residue 353, are located in this domain (Fig. 2A).

Domain 2 (i.e., residues 49–84 and 371–387) is elongated, mainly consists of a 3-stranded mixed β-sheet, and serves as

© Higher Education Press and Springer-Verlag Berlin Heidelberg 2010

Table 1 Statistics of data collection and refinement.

Data collection *				
space group	$P3_121$			
cell dimensions (Å)	a = b = 95.7	c = 117.0		
dataset	Native		Se-Met	
		λ1 (remote)	λ2 (peak)	λ3 (inf.)
wavelength used (Å)	1.000	0.96410	0.97866	0.97934
resolution range (Å)	50 (2.95)[a]–2.85	50 (3.11)–3.00	50 (3.11)–3.00	50 (3.11)–3.00
No. of unique refln	13204 (968)	12582 (887)	12949 (1135)	12934 (1116)
average redundancy	5.7 (5.6)	9.1 (5.5)	9.5 (6.2)	9.4 (5.8)
completeness (%)	88.5 (66.4)	95.3 (67.9)	98.2 (86.6)	98.0 (85.6)
I/σ (I)	30 (3.4)	39 (2.1)	44 (2.8)	43 (2.5)
R_{merge} [b] (%)	5.2 (31.6)	8.2 (33.9)	8.2 (32.2)	7.9 (33.5)
Refinement				
resolution (Å)	28.4–2.85			
$R_{working}$ [c] (%)/ No. of refln used	27.9/12016			
R_{free} [c] (%)/ No. of refln used	29.4/637			
No. of non-hydrogen atoms	3675			
average B factor (Å^2)	131.1 (90.5)[d]			
protein	131.1			
main chain	128.1			
side chain	134.2			
solvent	126.6			
r.m.s.d. from ideal values				
bond length (Å)	0.002			
bond angle (deg)	0.475			
dihedral angle (deg)	12.4			
ramachandran plot (%)[e]				
favored region	88.3			
allowed region	11.7			
disallowed region	0.0			
MolProbity score[f]	3.05 at 66th percentile (N = 3770, 2.602 − 3.102 Å)			

* All the data were collected at Photon Factory synchrotron facility (Tsukuba, Japan).

[a] Values in parentheses are for the highest resolution bin.

[b] $R_{merge} = \sum_{hkl}\sum_{i}|I_i - (I)|/|(I)|$, where I_i is the intensity for the ith measurement of an equivalent reflection with indices h,k,l.

[c] $R = \sum|Fo - Fc|/\sum|Fo|$, where Fo and Fc are the observed and calculated structure factors, respectively.

[d] Values in parentheses is the Wilson B factor calculated using the program Truncate (French and Wilson, 1978) in the CCP4 package (Bailey, 1994) and data in the resolution range of 4.0–2.86 Å.

[e] Calculated using Procheck (Laskowski et al., 1993).

[f] Calculated by MolProbity (Davis et al., 2007).

a bridge connecting domains 1 and 3 with domain 4.

Domain 3 (i.e., residues 176–225 and 272–346) is a sandwich-shaped, global, α/β/α domain. The central layer is composed of a 5-stranded antiparallel β-sheet (Fig. 1B). Each of the top and bottom layers contains three α helices. Domain 3 appears to be formed by two insertions to domain 1. Particularly, ^{3}α6, ^{3}β1, ^{3}β2, and ^{3}β3 of domain 3 appear to be a bent continuation of domain 1. The buried surface between domain 2 and domain 3 is 1280 Å^2 and is contributed by both the three-stranded β-sheet of domain 2 and ^{3}α1/^{3}α3 of

 © Higher Education Press and Springer-Verlag Berlin Heidelberg 2010

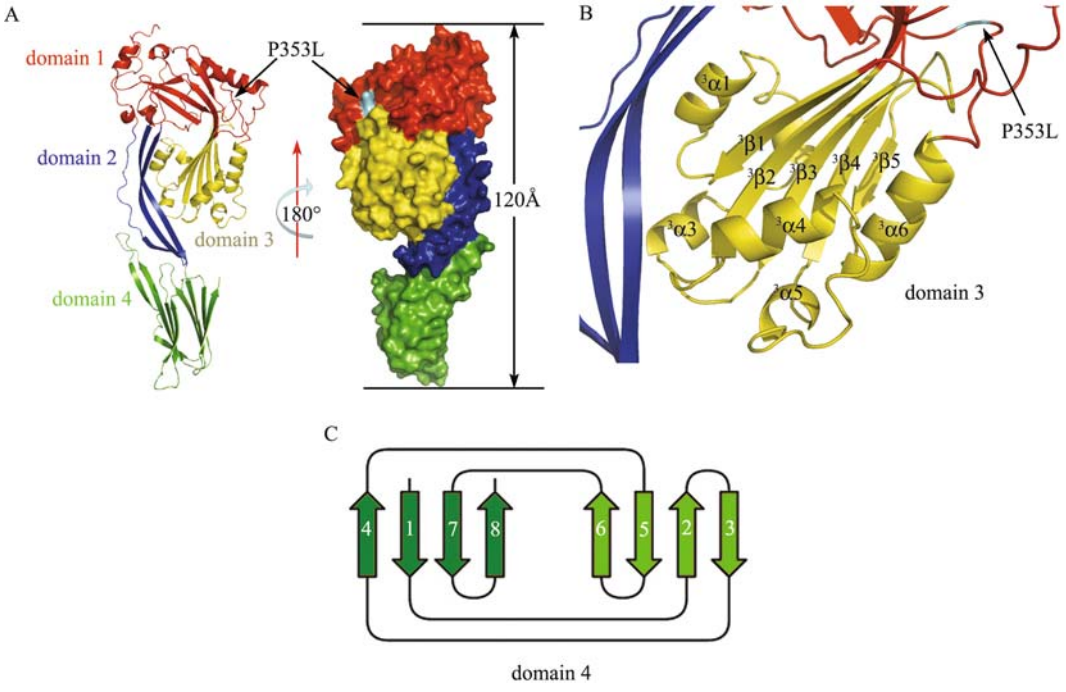

Figure 1. Overall structure of suilysin. (A) Ribbon diagram and molecular surface model of suilysin crystal structure with each domain colored differently. In addition, the mutation site, position 353, is colored in cyan. This figure was generated using the program Pymol (DeLano, 2002). (B) Sandwich-shaped domain 3 and relative position of the P353L mutation site. (C) Topology diagram of the β-sheets in domain 4.

domain 3. Because clusters of helices ^{3}α1/^{3}α2/^{3}α3 and ^{3}α4/^{3}α5/^{3}α6 were proposed to switch to a membrane spanning hairpin during pore oligomer formation, they were previously named as transmembrane hairpin 1 (TMH1) and TMH2, respectively (Shepard et al., 1998; Shatursky et al., 1999).

Distinct from other three domains, domain 4 (i.e., residues 388–497) is a continuously folded domain formed by the C terminal region of suilysin (Fig. 2A). It has a β-sandwich fold, which is composed of two β-sheets with a topology as shown in Fig. 1C. This fold appears to be an immunoglobulin fold, but its topology doesn't belong to any of the four types of classical immunoglobulin folds documented before (Bork et al., 1994). Two loops of domain 4 (residues 410–418 and 442–446) participate in a minor contact with domain 2.

Comparison with homologous structures

To put our suilysin crystal structure in a broader context, homologous structures of suilysin were analyzed by primary sequence alignment and 3D structure comparison.

A multiple alignment was performed with the program Clustalx (Thompson et al., 1997) among primary sequences of suilysin and 11 other homologous proteins whose sequence identities vary from 44% to 51% with suilysin (Fig. 2A). According to the conservativeness from the sequence alignment, every residue of suilysin was scored, and the scores were mapped to the suilysin 3D model as shown in Fig. 2B and 2C. The most conserved regions include a hydrophobic core of domain 1 and the above mentioned tryptophan-rich motif in domain 4. The hydrophobic core of domain 1 consists of Val150, Val154, Leu157 and Trp161 from hydrophobic side chains of the long amphipathic helix ^{1}α3 and Leu130, Tyr228, Val268, Tyr270, Pro356, Ile357 and Pro99 from the β-sheet of domain 1 (Fig. 2C).

The members of CDC family show over 40% sequence identity over their common region corresponding to domains 1–4, suggesting that they share a similar 3D structure. Comparison of the suilysin crystal structure with those of other CDC family members (PFO, ILY, and ALO) confirmed this prediction. Domains 1–3 of suilysin were superimposed to PFO (PDB file: 1PFO) with a root mean square deviation (rmsd) of 1.5 Å for 256 pairs of Cα atoms, ILY (PDB file: 1S3R, chain A) with an rmsd of 1.5 Å for 278 pairs of Cα atoms, and ALO (PDB file: 3CQF, chain A) with an rmsd of 1.7 Å for 283 pairs of Cα atoms (all using a 3 Å cutoff). Similarly, for superimposed domain 4, the rmsd between suilysin and PFO is 1.03 Å for 95 Cα pairs, it is 1.04 Å for 110 Cα pairs between suilysin and ILY, and it is 1.05 Å for 98 pairs of Cα atoms between suilysin and ALO. Therefore, among available CDC homolog structures, the folding differences between their domains 1–3 and domain 4 separately are marginal. However,

© Higher Education Press and Springer-Verlag Berlin Heidelberg 2010

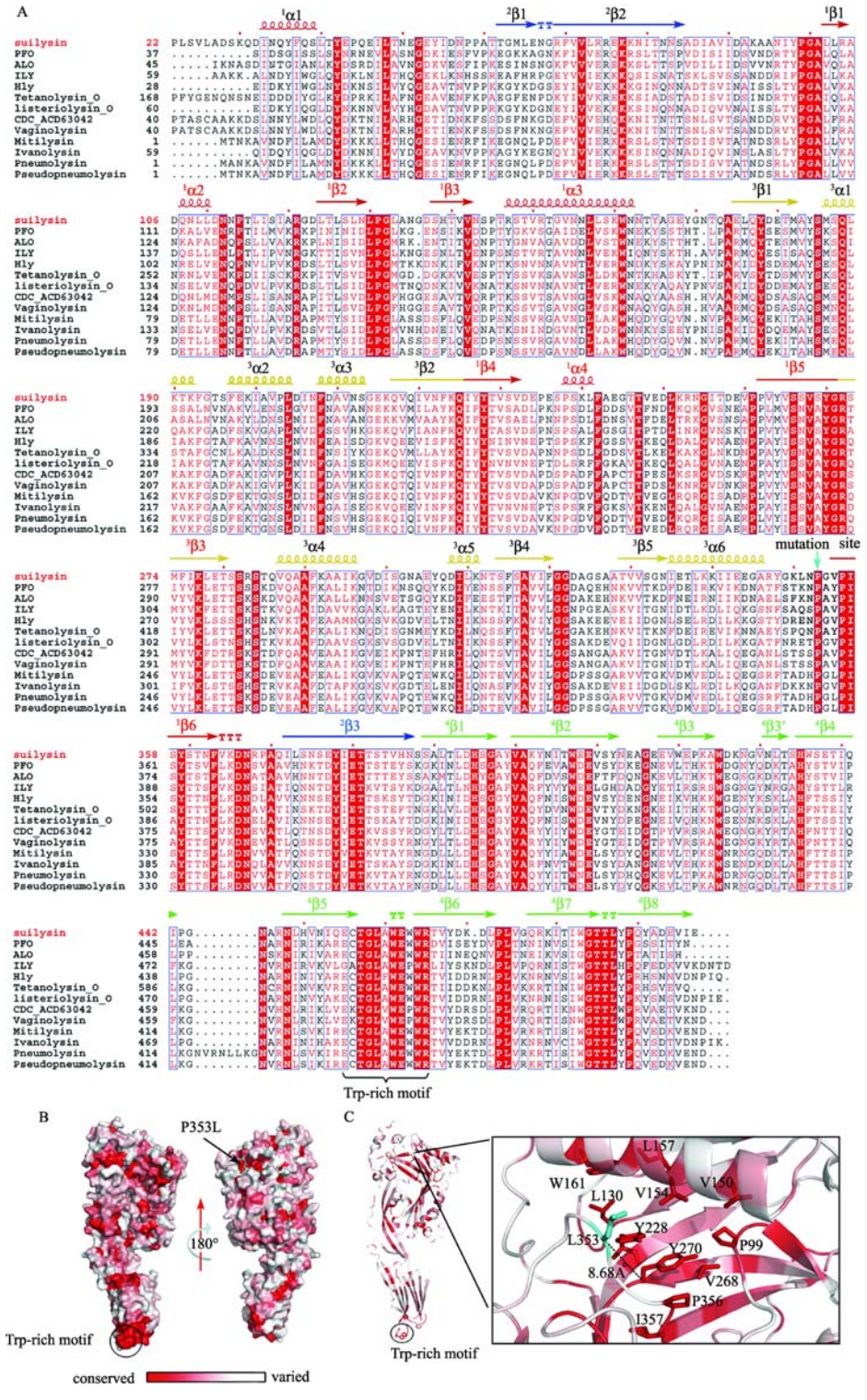

Figure 2. Amino acid conservation analysis on primary sequence and 3D level. (A) Multiple alignment of primary sequences among suilysin and 11 other homologous proteins, including PFO (PDB accession#: 1PFO_A), ALO (3CQF_A), ILY (1M3J_A), tetannlysin_O (GenBank accession #: ZP_02620072), Hly (ACE82237), listeriolysin_O (ABS57173), vaginolysin (ACD39459), mitilysin (ABK58690), ivanolysin (P31831), pneumolysin (ABO21347) and pseudopneumolysin (ACJ76902). Residue 353 that was mutated to Leu in our suilysin crystal structure and the Trp-rich motif are marked with an arrow and a brace, respectively. The alignment was performed with the program ClustalX (Thompson et al., 1997). The color code for secondary structure elements from different domains is the same as Fig. 1A. (B) Molecular surface representation. (C) Conserved hydrophobic core of domain 1. Position 353 was colored in cyan. For (B) and (C), Conservation scores for every residues based on the 12-sequence alignment in (A) were calculated by using the program ClustalX (Thompson et al., 1997) and mapped to the 3D structure of suilysin. Absolutely conserved residues (i.e., scored 100) were colored red, those less conserved (scored 25 or lower) were colored white, and others in between.

there is a clear hinge-bending motion between the domains 1–3 and domain 4 among these crystal structures. A hinge-bending angle is defined as the following: first, domains 1–3 from two structures are superimposed; subsequently, the swing rotation angle required to superimpose domain 4 would be the hinge-bending angle. While the hinge-bending angle between ILY and suilysin is about 40°, it is about 15° between ALO and suilysin, and about −10° between PFO and suilysin (Fig. 3). Among them, ILY is the most bent one, and PFO is the least bent one. Another significant structural variation among the available crystal structures of CDC homologs is their Trp-rich motif in domain 4 located at the tip of the elongated 3D structure. During refinement of suilysin, this motif was built manually. This structural difference will be discussed in more detail later.

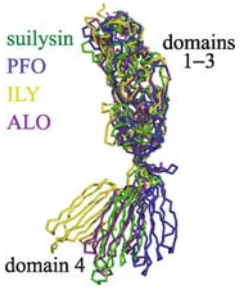

Figure 3. Structure comparison of suilysin, PFO (1PFO), ILY (1S3R, chain A) and ALO (3CQF, chain A). Cα traces of these crystal structures were superimposed based on their domains 1–3. The orientation is similar to the right panel of Fig. 1A.

A search using the Dali website (http://ekhidna.biocenter.helsinki.fi/dali_server) for homologous folding confirmed one significant hit beyond the classic CDC family members, the bacterial membrane attack complex/perforin-like protein, Plu-MACPF from *P. luminescens* (PDB file: 2PQ2) (Rosado et al., 2007). The structure homology between suilysin and Plu-mACPF is fairly good, with 1.9 Å rmsd for 62 Cα pairs (using a 3 Å cutoff); and the homology is high in the domains 1 and 3. On the other hand, the corresponding sequence homology is lower than detectable level, the signature motif of MACPF (Y/W-G-T/S-H-F/Y) is not present in the CDC family (Ponting, 1999), and the 3D structure in this region is different between the two families. In vertebrates, members of the MACPF family are part of complement system and form oligomeric pores that lyse bacteria or kill virus-infected cells. The significant structural homology between the two families further supports that the pore formation by suilysin and other CDC member is mediated by the domains 1 and 3 (Tilley et al., 2005). Interestingly, the only three conserved residues between the CDC and MACPF families are Gly271, Gly321 and Gly322 (in suilysin number), all of which are located in the bending region of the connected β-sheet between domains 1 and 3. They are speculated to play a hinge role during conformational changes. It is conceivable that when the TMH1 cluster moves away from the core of the so called CDC/MACPF domain (i.e., domains 1 and 3 in CDC) to form the pore-lining β-sheet barrel, the bending β-sheet of the core itself will collapse into a more compact β sandwich structure.

Crystal packing

In the suilysin crystal, the largest inter-molecular pair-wise contact surface was 1200 $Å^2$ (summation from both molecules). This contact was observed between two suilysin molecules related by a crystallographic dyad symmetry (i.e., the one at [110] direction), and was mediated by ^{3}α6 and ^{3}β5 (i.e., residue 328–350) of domain 3 (Fig. 4A). According to a survey of PDB, an interface of 1200 $Å^2$ of buried solvent-accessible area is typical for protein crystal packing (Bahadur et al., 2004). Twenty-nine (55%) out of 53 atoms involved in the interface from one suilysin molecule are carbon-containing group, which is also in line with the typical crystal dimer instead of a biological dimer. The number of atoms (53)

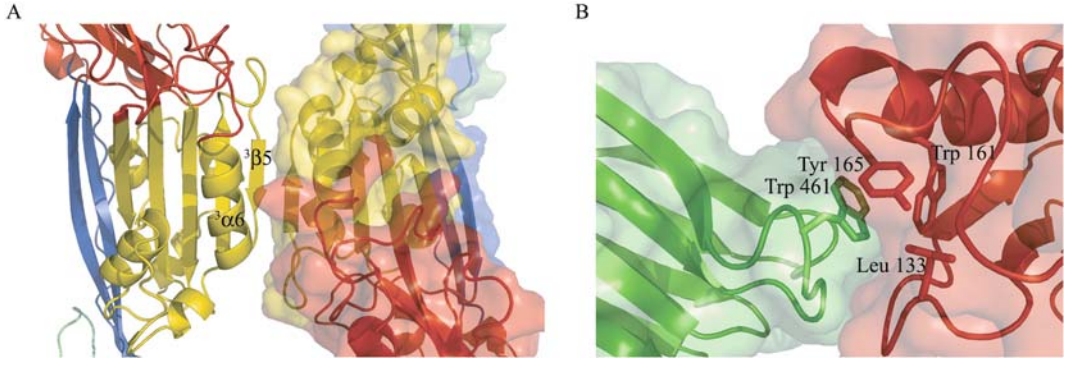

Figure 4. Crystal contacts between neighboring asymmetric units. (A) Crystal contact mediated by a dyad symmetry and involving ^{3}α6 and ^{3}β5. (B) Trp-rich motif involved in hydrophobic contact. The color code is the same as in Fig. 1A.

© Higher Education Press and Springer-Verlag Berlin Heidelberg 2010

contributing to the crystal packing interface from each protein molecule is actually smaller than the average number, 80, from the survey. Therefore, this observed crystal interface is unlikely to represent a long-lived assembly in solution (Bahadur et al., 2004). This is consistent with the monomeric form of suilysin in solution judged from size exclusion chromatography results (data not shown).

In the homologous PFO and ILY crystals, $^{3}\alpha6$ is not involved in any crystal contact. In the ALO crystal structure, its $^{3}\alpha6$ only participates in a minor (ca. total 414 Å^2) crystal packing while its $^{3}\beta5$ is mobilized. Thus, the 1200 Å^2 interface observed in suilysin crystal is likely to be an artifact of crystallization. Taken together, conserved large monomer-monomer contact is not observed among available CDC crystals; a similar conclusion was also recently reported on the ALO structure (Bourdeau et al., 2009).

DISCUSSION

Members of the CDC family share two basic functions. First, they bind to the membrane of the target cell via specific interactions between the carboxyl-terminal 4th domain and receptors on the membrane, including cholesterol. Second, in response to the membrane binding, they oligomerize, change conformation in the amino-terminal portion, and form transmembrane pores (Rossjohn et al., 1997; Giddings et al., 2004; Polekhina et al., 2005; Tilley et al., 2005). Our suilysin crystal structure provides a new view point to the increasingly intensified discussion on the mechanisms of these functions. It is conceivable that these conserved functions are associated with some conserved structural features of the CDC members. Interestingly, highly conserved primary sequences are mapped into two regions in the 3D structure of suilysin, the hydrophobic core in the N-terminal portion and the Trp-rich motif at the tip of the C-terminal 4th domain (Fig. 2B and 2C).

The Trp-rich motif has long been speculated to be involved in cholesterol binding. Variation in this motif has been associated with functional difference among CDC members (Nagamune et al., 2004; Polekhina et al., 2005; Soltani et al., 2007b; Bourdeau et al., 2009). However, in a recent study on ILY and PFO, it was shown that instead of mediating membrane insertion of the Trp-rich motif, cholesterol triggers other three small loops (L1–L3, Fig. 5) of domain 4 to insert into the membrane (Soltani et al., 2007b). Considering the fact that L1–L3 loops in PFO and ILY adopt nearly identical conformations, a question to be addressed is why the L1–L3 loops cannot facilitate ILY binding to a cholesterol-rich membrane in a way similar to what they do in PFO. It has been shown that ILY can gain the ability of binding to non-human cells, thus independent of CD59, if its Trp-rich motif is replaced with that of PFO (Nagamune et al., 2004). In addition, the insertion of ILY L1–L3 loops to membrane can be disrupted by one point mutation (e.g., W491A in ILY) in the Trp-rich motif (Soltani et al., 2007a). Therefore, the amino acid sequence in the Trp-rich motif seems indeed to influence the membrane association of domain 4, albeit the mechanism remains to be revealed.

One simple explanation would be that a sequence variation in the Trp-rich motif triggers its conformational change and thus results in a functional difference. Nevertheless, our suilysin structure challenges such a view. Although the crystal structure of suilysin possesses an ILY-like conformation in the Trp-rich motif, suilysin does not function in a receptor-dependent manner like ILY. In our suilysin crystal structure, the Trp-rich motif in domain 4 adopts an extended conformation similar to that observed in the ILY crystal structure (Fig. 5). In contrast, this motif is folded back onto the domain 4 β-sheet in the PFO and ALO crystal structures, both of which bind to the membrane in a receptor-independent manner. At the primary sequence level, suilysin has a tryptophan residue at the position 463, which is conserved in PFO (Trp466) and ALO (Trp477), while ILY has a Pro residue at the corresponding position (Fig. 2A). Therefore, the conformational difference observed between the ILY and PFO is unlikely to be simply caused by sequence variation within the motif. Furthermore, our new structure data suggest that conformation of the Trp-rich motif alone is insufficient to determine the mode how a CDC protein would interact with the membrane.

Nevertheless, caution should be taken in regards to interpreting a crystal structure. For example, in suilysin crystal

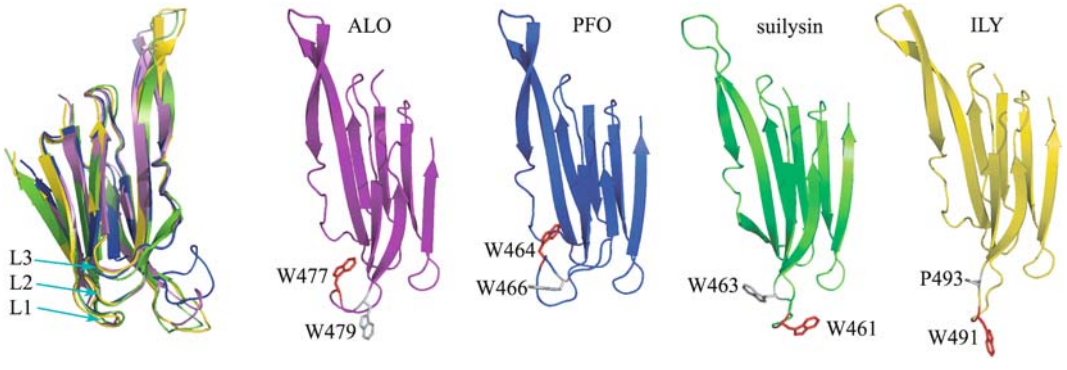

Figure 5. Comparison of the Trp-rich loops as well as domains 4 from four crystal structures of CDC family members.

 © Higher Education Press and Springer-Verlag Berlin Heidelberg 2010

structure, the exposed hydrophobic side chains from the Trp-rich loop mediate a crystal packing. In particular, Trp461 sitting at the tip of the Trp-rich loop interacts with Leu133, Trp161 and Tyr165 of a neighboring suilysin molecule in the crystal lattice (Fig. 4B). Regarding ILY, the open conformation of its Trp-rich loop does not contribute directly to crystal packing. If the conformation of suilysin Trp-rich motif was a solo result of the crystal contact, it would mean that this undecapeptide was so flexible that it is easy to adopt an environment-induced conformation. In our opinion, such a flexibility of the Trp-rich motif would difficult to consolidate with its key role in affecting membrane insertion of L1–L3 loops. We hope that the crystal structure of suilysin will serve as an extra reference in investigation of the role of the Trp-rich motif in the membrane association mechanism in the future.

In our crystal, the suilysin variant contains a P353L point mutation. This position is absolutely conserved to be proline among all CDC homolog proteins that were included in the alignment shown in Fig. 2A. This loop varies its conformation among the currently available CDC crystal structures. In suilysin, residue 353 is located close to the conserved hydrophobic core in domain 1. For example, the Cα atom distance between Leu353 and Tyr270 from the core is about 8 Å (Fig. 2C). In addition, the mutation site resides in an inter-domain loop connecting domains 1 and 3 (Fig. 2A). It is C-terminal to the region of ^{3}α6 and ^{3}β5 that was previously identified as a switch apparatus during oligomerization (Ramachandran et al., 2004; Tilley et al., 2005). We speculate that a modified flexibility of this switch region may (partially) contribute to the better crystal quality of the P353L mutant over the WT since its N-terminal region is directly involved in crystal packing. Furthermore, a mutation at such a position may either disturb structure of the conserved domain 1 core or influence the dynamics of domain 3 relative to domain 1. Indeed, this P353L point mutation results in a loss of hemolytic ability but a gain of erythrocyte aggregation (H.D. unpublished result).

MATERIALS AND METHODS

Protein expression, purification, and crystallization

Recombinant proteins of WT and P353L variant suilysin from *S. suis* were expressed as an N-terminal GST fusion protein using pGEX-6p-1 vector (Amersham Pharmacia Biotech) in the *E. coli* BL21 (DE3) strain, and purified with GST-affinity chromatography and Resource Q (GE healthcare) ion exchange chromatography. The GST tag was removed using PreScission protease (Amersham Pharmacia Biotech) before crystallization.

Crystals of suilysin was grown using the hanging drop method at 16°C. The protein sample was stored at about 12 mg/mL concentration in 200 mM NaCl, 20 mM HEPES (pH 7.2), and 5% (*v/v*) 1,2,3-heptanetriol; and it was mixed 6:4 with the precipitant solution of 18% (*w/v*) polyethylene glycol (PEG) 3350, 0.12 M sodium citrate (pH 7.0), and 2% (*v/v*) 1,1,1,3,3,3-hexafluoro-2-propanol. A selenium-methionine (Se-Met) derivative protein sample was similarly expressed, purified and crystallized.

Data collection

Both the native crystal and its Se-Met derivative were dehydrated prior to diffraction data collection. First, the crystals were soaked in the mother liquid supplemented with 5% (*v/v*) glycerol for 20 min; then the concentration of glycerol was increased by 5% every 20 min until the final concentration of glycerol reached 20%. The crystal was then cooled in a nitrogen stream (170 K) for data collection. Diffraction data were collected up to 2.85 Å resolution for the native crystal and to 3.0 Å for the se-Met derivative crystal on the beamline 17A at the Photon Factory synchrotron facility (Tsukuba, Japan). The diffraction data were indexed, integrated, and scaled using the program package HKL2000 (Otwinowski and Minor, 1997).

Structure determination

Phases of the crystal structure of suilysin were determined using the multi-wavelength anomalous dispersion (MAD) method. Three of the five selenium atoms were located using the program ShelxD (Schneider and Sheldrick, 2002). Coordinates of these selenium atoms were then input into the program Phenix-autosol (Adams et al., 2002) for initial phase determination. The mean figure of merit (FOM) was 0.51 for total data. Then the phases were combined with structure factors obtained from the native crystal. Initial molecular replacement attempt was not successful. However, we were able to position the domains 1–3 and 4 of ILY (PDB ID: 1S3R) separately into the electron density map calculated with the initial MAD phases. Refinement started from a model of 44% completeness and a 47% R-free; and the quality of the initial electron density map was low in many regions. The program Phenix-refine (Adams et al., 2002) was used through the refinement, and the model was gradually completed by manual model building using the graphic program Coot (Emsley and Cowtan, 2004). Because of the limited resolution, restrained isotropic individual B factor refinement was used. TLS refinement was performed in four TLS groups (i.e., residues 32–94, 95–291, 292–383, and 384–499) suggested by the TLSMD sever (http://skuld.bmsc.washington.edu/~tlsmd/) (Painter and Merritt, 2006). R-free was used to monitor the refinement process, and the quality of the geometry of the final model was verified using the program ProCheck (Laskowski et al., 1993). The final rmsd of bonded B factors was constrained to 10.8 Å^2. In the final model, residues 1–31, 243, and 244 were missing due to poor quality of the electron density in these regions. Structure comparison and analysis was performed with the program EdPDB (Zhang and Matthews, 1995).

Coordinates deposition

Coordinates of the refined model of suilysin and its experimental structural factors have been deposited to the RCSB Protein Data Bank (http://www.rcsb.org/pdb/). The access ID is 3HVN.

ACKNOWLEDGEMENTS

We are very grateful to staff members of the Structural Biology Core Facility in the Institute of Biophysics, Chinese Academy of Sciences

© Higher Education Press and Springer-Verlag Berlin Heidelberg 2010

(CAS), for their excellent technical assistance, especially to Ms. Ning Hao, Mr. Zhongnian Zhou, Ms. Meirong Zhang, Mr. Jianhui Li, Mr. Yi Han, and Ms. Xiaoxia Yu. We also thank Dr. Simon Terzyan for helpful discussion. This work was supported by the National Programs for High Technology Research and Development Program (863 Program) No. 2006AA02A322 to X.L., the CAS grant KSCX2-YW-05 to Z.R, the Project of Protein Studies (CAS) grant 2006CB10903, and National Basic Research Program (973 Program) No. 2007CB914304.

ABBREVIATIONS

ALO, anthrolysin O; CDC, cholesterol-dependent cytolysin; FOM, figure of merit; MAD, multiple-wavelength anomalous dispersion; ILY, intermedilysin; MACPF, membrane attack complex/performing; PFO, perfringolysin O; rmsd, root mean square deviation; TMH, transmembrane hairpin

REFERENCES

Adams, P.D., Grosse-Kunstleve, R.W., Hung, L.W., Ioerger, T.R., McCoy, A.J., Moriarty, N.W., Read, R.J., Sacchettini, J.C., Sauter, N.K., and Terwilliger, T.C. (2002). PHENIX: building new software for automated crystallographic structure determination. Acta Crystallogr D Biol Crystallogr 58, 1948–1954.

Bahadur, R.P., Chakrabarti, P., Rodier, F., and Janin, J. (2004). A dissection of specific and non-specific protein-protein interfaces. J Mol Biol 336, 943–955.

Bailey, S. (1994). The CCP4 suite: programs for protein crystallography. Acta Crystallographica D50, 760–763.

Bork, P., Holm, L., and Sander, C. (1994). The immunoglobulin fold. Structural classification, sequence patterns and common core. J Mol Biol 242, 309–320.

Bourdeau, R.W., Malito, E., Chenal, A., Bishop, B.L., Musch, M.W., Villereal, M.L., Chang, E.B., Mosser, E.M., Rest, R.F., and Tang, W. J. (2009). Cellular functions and X-ray structure of anthrolysin O, a cholesterol-dependent cytolysin secreted by Bacillus anthracis. J Biol Chem.

Davis, I.W., Leaver-Fay, A., Chen, V.B., Block, J.N., Kapral, G.J., Wang, X., Murray, L.W., Arendall, W.B., 3rd, Snoeyink, J., Richardson, J.S., *et al*. (2007). MolProbity: all-atom contacts and structure validation for proteins and nucleic acids. Nucleic Acids Res 35, W375–383.

DeLano, W.L. (2002). The PyMOL Molecular Graphics System. DeLano Scientific, Palo Alto, CA, USA.

Emsley, P., and Cowtan, K. (2004). Coot: model-building tools for molecular graphics. Acta Crystallogr D Biol Crystallogr 60, 2126–2132.

French G.S. and Wilson K.S. (1978). On the treatment of negative intensity observations. Acta Cryst A34, 517–525.

Giddings, K.S., Johnson, A.E., and Tweten, R.K. (2003). Redefining cholesterol's role in the mechanism of the cholesterol-dependent cytolysins. Proc Natl Acad Sci U S A 100, 11315–11320.

Giddings, K.S., Zhao, J., Sims, P.J., and Tweten, R.K. (2004). Human CD59 is a receptor for the cholesterol-dependent cytolysin intermedilysin. Nat Struct Mol Biol 11, 1173–1178.

Gottschalk, M., and Segura, M. (2000). The pathogenesis of the meningitis caused by Streptococcus suis: the unresolved questions. Vet Microbiol 76, 259–272.

Jacobs, A.A., Loeffen, P.L., van den Berg, A.J., and Storm, P.K. (1994). Identification, purification, and characterization of a thiol-activated hemolysin (suilysin) of Streptococcus suis. Infect Immun 62, 1742–1748.

Laskowski, R.A., MacArthur, M.W., Moss, D.S., and Thornton, J.M. (1993). PROCHECK: a program to check the stereochemical quality of protein structures. J Appl Crystallogr 26, 283–291.

Matthews, B.W. (1968). Solvent contents of protein crystals. J Mol Biol 33, 491–497.

Nagamune, H., Ohkura, K., Sukeno, A., Cowan, G., Mitchell, T.J., Ito, W., Ohnishi, O., Hattori, K., Yamato, M., Hirota, K., *et al*. (2004). The human-specific action of intermedilysin, a homolog of streptolysin O, is dictated by domain 4 of the protein. Microbiol Immunol 48, 677–692.

Nagamune, H., Ohnishi, C., Katsuura, A., Fushitani, K., Whiley, R.A., Tsuji, A., and Matsuda, Y. (1996). Intermedilysin, a novel cytotoxin specific for human cells secreted by Streptococcus intermedius UNS46 isolated from a human liver abscess. Infect Immun 64, 3093–3100.

Otwinowski, Z., and Minor, W. (1997). Processing of X-ray diffraction data collected in oscillation mode. Methods Enzymol 276, 307–326.

Painter, J., and Merritt, E.A. (2006). Optimal description of a protein structure in terms of multiple groups undergoing TLS motion. Acta Crystallogr D Biol Crystallogr 62, 439–450.

Polekhina, G., Giddings, K.S., Tweten, R.K., and Parker, M.W. (2005). Insights into the action of the superfamily of cholesterol-dependent cytolysins from studies of intermedilysin. Proc Natl Acad Sci U S A 102, 600–605.

Ponting, C.P. (1999). Chlamydial homologues of the MACPF (MAC/perforin) domain. Curr Biol 9, R911–913.

Ramachandran, R., Tweten, R.K., and Johnson, A.E. (2004). Membrane-dependent conformational changes initiate cholesterol-dependent cytolysin oligomerization and intersubunit beta-strand alignment. Nat Struct Mol Biol 11, 697–705.

Rosado, C.J., Buckle, A.M., Law, R.H., Butcher, R.E., Kan, W.T., Bird, C.H., Ung, K., Browne, K.A., Baran, K., Bashtannyk-Puhalovich, T. A., *et al*. (2007). A common fold mediates vertebrate defense and bacterial attack. Science 317, 1548–1551.

Rossjohn, J., Feil, S.C., McKinstry, W.J., Tweten, R.K., and Parker, M. W. (1997). Structure of a cholesterol-binding, thiol-activated cytolysin and a model of its membrane form. Cell 89, 685–692.

Rossjohn, J., Polekhina, G., Feil, S.C., Morton, C.J., Tweten, R.K., and Parker, M.W. (2007). Structures of perfringolysin O suggest a pathway for activation of cholesterol-dependent cytolysins. J Mol Biol 367, 1227–1236.

Schneider, T.R., and Sheldrick, G.M. (2002). Substructure solution with SHELXD. Acta Crystallogr D Biol Crystallogr 58, 1772–1779.

Shatursky, O., Heuck, A.P., Shepard, L.A., Rossjohn, J., Parker, M. W., Johnson, A.E., and Tweten, R.K. (1999). The mechanism of membrane insertion for a cholesterol-dependent cytolysin: a novel paradigm for pore-forming toxins. Cell 99, 293–299.

Shepard, L.A., Heuck, A.P., Hamman, B.D., Rossjohn, J., Parker, M. W., Ryan, K.R., Johnson, A.E., and Tweten, R.K. (1998). Identification of a membrane-spanning domain of the thiol-activated pore-forming toxin Clostridium perfringens perfringolysin O: an alpha-helical to beta-sheet transition identified by fluorescence spectroscopy. Biochemistry 37, 14563–14574.

 © Higher Education Press and Springer-Verlag Berlin Heidelberg 2010

Soltani, C.E., Hotze, E.M., Johnson, A.E., and Tweten, R.K. (2007a). Specific protein-membrane contacts are required for prepore and pore assembly by a cholesterol-dependent cytolysin. J Biol Chem 282, 15709–15716.

Soltani, C.E., Hotze, E.M., Johnson, A.E., and Tweten, R.K. (2007b). Structural elements of the cholesterol-dependent cytolysins that are responsible for their cholesterol-sensitive membrane interactions. Proc Natl Acad Sci U S A 104, 20226–20231.

Thompson, J.D., Gibson, T.J., Plewniak, F., Jeanmougin, F., and Higgins, D.G. (1997). The CLUSTAL_X windows interface: flexible strategies for multiple sequence alignment aided by quality analysis tools. Nucleic Acids Res 25, 4876–4882.

Tilley, S.J., Orlova, E.V., Gilbert, R.J., Andrew, P.W., and Saibil, H.R. (2005). Structural basis of pore formation by the bacterial toxin pneumolysin. Cell 121, 247–256.

Tweten, R.K. (2005). Cholesterol-dependent cytolysins, a family of versatile pore-forming toxins. Infect Immun 73, 6199–6209.

Tweten, R.K., Parker, M.W., and Johnson, A.E. (2001). The cholesterol-dependent cytolysins. Curr Top Microbiol Immunol 257, 15–33.

Zhang, X., and Matthews, B.W. (1995). EDPDB: A multifunctional tool for protein structure analysis. J Appl Crystallogr 28, 624–630.

© Higher Education Press and Springer-Verlag Berlin Heidelberg 2010